# Observation of Berry's Geometrical Phase in Electron Diffraction from a Screw Dislocation

D. M. Bird[1] and A. R. Preston[2]

[1]School of Physics, University of Bath, Bath BA2 7AY, United Kingdom
[2]H.H. Wills Physics Laboratory, University of Bristol, Bristol BS8 1TL, United Kingdom

The equations which govern high-energy electron diffraction in a deformed crystal lattice are shown to be equivalent to a Schrödinger equation with a time-dependent Hamiltonian. If the lattice planes are not strongly distorted, as in the long-ranged strain field of a dislocation, this time variation is slow and adiabatic theory can be used. The effects of Berry's geometrical phase are then observed in the bending of two-beam diffraction fringes as a screw dislocation is crossed.

A great amount of interest has been generated by Berry's discovery[1] of a geometrical phase factor associated with the adiabatic transport of a quantum system around a closed circuit in some parameter space. A number of experiments have been reported which demonstrate the effects of this phase, including observations on photons,[2] neutrons,[3] nuclear spins,[4] and moleculer energy levels.[5] Here we show that the equations which govern high-energy electron diffraction from a continuously deformed crystal can be expressed in the form of a time-dependent Schrödinger equation whose Hamiltonian varies as the lattice planes bend. In weakly deformed regions this variation is slow and adiabatic approximations can be used. The resulting diffraction patterns provide a particularly straightforward and graphic demonstration of Berry's phase, and a first observation of the phase for electrons.

The system we consider is shown in Fig. 1. A screw dislocation with Burger's vector $\mathbf{b}$ is threaded through the center of a thin crystalline slab of thickness $t$. The surfaces of the crystal lie in the planes $z = -t/2$ and $z = t/2$ and the fast electrons, with wave vector $\mathbf{k}$, are incident nearly parallel to $z$. If the dislocation lies along a diad, with a second diad perpendicular to this (as in graphite, see below), the long-ranged displacement field becomes $\Delta\mathbf{r} = (\mathbf{b}/2\pi)\tan^{-1}(z/\lambda R)$, where $R$ is the distance, parallel to the surface, from the core and $\lambda$ is an anisotropy parameter.[6] The diffraction is governed by the Howie-Whelan equations,[7] which can be expressed in the form

$$\begin{bmatrix} W & Ue^{i\mathbf{g}\cdot\Delta\mathbf{r}} \\ Ue^{-i\mathbf{g}\cdot\Delta\mathbf{r}} & -W \end{bmatrix} \begin{bmatrix} A_0 \\ A_{\mathbf{g}} \end{bmatrix} = -2ik\frac{d}{dz}\begin{bmatrix} A_0 \\ A_{\mathbf{g}} \end{bmatrix}. \qquad (1)$$

A number of standard approximations in electron diffraction theory are made in the derivation of (1).

*Forward-scattering approximation.*[7]—This is an excellent approximation at the high energies ($> 100$ keV) considered. It reduces the time-independent equation which governs the diffraction to an equation which is first order in $z$ and leaves (1) in the form of a *time-dependent* Schrödinger equation where $z$, the depth in

the crystal, takes the place of time.

*Two-beam approximation.*[7]—Only waves corresponding to reciprocal-lattice vectors $\mathbf{0}$ and $\mathbf{g}$ are included. $A_0$ and $A_{\mathbf{g}}$ represent the amplitudes of these waves, so that the total wave field becomes $A_0(z)e^{i\mathbf{k}\cdot\mathbf{r}} + A_{\mathbf{g}}(z)e^{i(\mathbf{k}+\mathbf{g})\cdot\mathbf{r}}$. Equation (1) then describes the dynamical coupling between the straight-through and diffracted waves. For simplicity we assume that $\mathbf{g}$ lies in the plane of the specimen (symmetric Laue geometry), and parallel to $\mathbf{b}$. The two-beam approximation is valid for relatively weak diffraction situations where the electrons are incident close to the Bragg condition for only one $\mathbf{g}$. The deviation away from the exact Bragg condition at $\mathbf{K} = -\mathbf{g}/2$ is described by $W = \mathbf{g}\cdot(\mathbf{K}+\mathbf{g}/2)$, where $\mathbf{K}$ is the transverse component of $\mathbf{k}$.

*Deformable ion approximation.*[7,8]—In a perfect crystal $U$ is the gth Fourier component, $U_{\mathbf{g}}$, of the periodic potential. If the crystal is deformed with a displacement
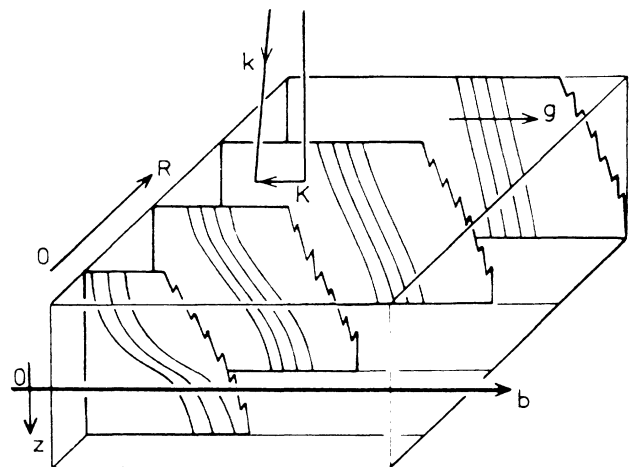


FIG. 1. The diffraction geometry. The distortion of the lattice planes is shown for a number of columns on the far side of the dislocation. On the near side the distortion is similar but in the opposite direction.

field $\Delta r(r)$ then at each point the crystal is taken to be perfect, but with a shift of origin which gives rise to an extra phase factor $\exp(-i g \cdot \Delta r)$ in $U_g$. This approximation is valid provided $g \cdot \Delta r$ is a slowly varying function of $r$, which is the case away from the dislocation core. We ignore any effects of absorption, and so $U$ in (1) is real and positive.

*Column approximation.*[7,8]— Although $z$ is a dynamical variable in (1), $R$ is not and only appears as a parameter. The crystal is imagined to be divided into columns at different distances $R$ from the dislocation core. Each column is assumed to be sufficiently wide for it to scatter independently of the others, while being narrow enough for the displacement to be constant across its width. As above, the column approximation is valid for slowly varying displacement fields.[8] The bending of the diffracting planes at various values of $R$ is sketched in Fig. 1.

*Neglect of surface relaxation and twisting.*— The expression for $\Delta r$ is valid in an infinite crystal and is assumed to remain so in a thin slab. Graphite is a suitable material for experimental work because dislocations with $b$ in the basal plane can be observed running through specimens with large areas of uniform thickness, where the surfaces cannot twist in response to the strain.

Our aim is to calculate the diffracted intensity, $|A_g|^2$, as a function of $W$ and $R$ for various values of $U$, $g \cdot b$, and $t$. This information can be observed in a *single* large-angle, dark field, convergent-beam electron diffraction pattern[9,10] of the type shown in Fig. 2(a). As in a standard convergent-beam pattern, each point represents the diffraction into the chosen reflection $g$ from a different incident orientation, but because the electron beam is focused either above or below the specimen, each point also arises from a different part of the crystal. In the present case, the real and reciprocal-space aspects of the pattern separate out because two-beam diffraction depends only on the component of $K$ parallel to $g$, while the curvature of the planes varies only in the direction perpendicular to $b$ and $g$. The fringes observed in Fig. 2(a) therefore reflect the variation of diffracted intensity

with incident orientation (i.e., $W$), while along their length they move in real space (i.e., $R$) across the crystal. A screw dislocation with $b = \frac{1}{3} a [11\bar{2}0]$ runs horizontally through the center of Fig. 2(a). The main feature of interest here is the bending of the two-beam fringes as the dislocation is approached. We will see that this phenomenon has a straightforward interpretation in terms of the geometrical phase. The interesting structure nearer the core has also received attention[10] but here the planes are bending too rapidly for an adiabatic approximation to be useful.

The substitutions $\beta = Ut/2k$, $x = Wt/2k$, $y = 2\lambda R/t$, and $\theta = 2z/t$ bring (1) into a dimensionless form

$$\frac{1}{2} \begin{bmatrix} x & \beta e^{i\phi} \\ \beta e^{-i\phi} & -x \end{bmatrix} \begin{bmatrix} A_0 \\ A_g \end{bmatrix} = -i \frac{d}{d\theta} \begin{bmatrix} A_0 \\ A_g \end{bmatrix}, \qquad (2)$$

where $\phi(\theta) = (g \cdot b/2\pi)\tan^{-1}(\theta/y)$ and where $\theta$ runs from $-1$ to $1$. The instantaneous, parallel-transported[11,12] eigenstates (Bloch waves, in electron diffraction theory) of this Hamiltonian are

$$C^\pm(\theta) = \frac{e^{\pm i\gamma}}{\sqrt{2}} \begin{bmatrix} e^{i\phi/2}\left(1 \pm \dfrac{x}{(x^2+\beta^2)^{1/2}}\right)^{1/2} \\ \pm e^{-i\phi/2}\left(1 \mp \dfrac{x}{(x^2+\beta^2)^{1/2}}\right)^{1/2} \end{bmatrix}$$

with corresponding eigenvalues $\pm \frac{1}{2}(x^2+\beta^2)^{1/2}$. The phase $\gamma$ arises from the parallel-transport condition and is given by

$$\gamma(\theta) = -\frac{1}{2} \frac{x}{(x^2+\beta^2)^{1/2}} \int_{-1}^{\theta} \dot\phi, \qquad (3)$$

where the overdot represents differentiation with respect to $\theta$. Equation (2) is essentially identical to the spin-$\frac{1}{2}$ system considered by Berry,[1,12] with (3) representing the geometrical phase. There are, however, two significant differences. First, $\theta$ runs over a finite interval, and so the change in the Hamiltonian cannot be truly adiabatic, i.e., infinitely slow. Our "time" dependence appears only in $\phi$, in the combination $\theta/y$, and so $1/y$ acts as a slow-
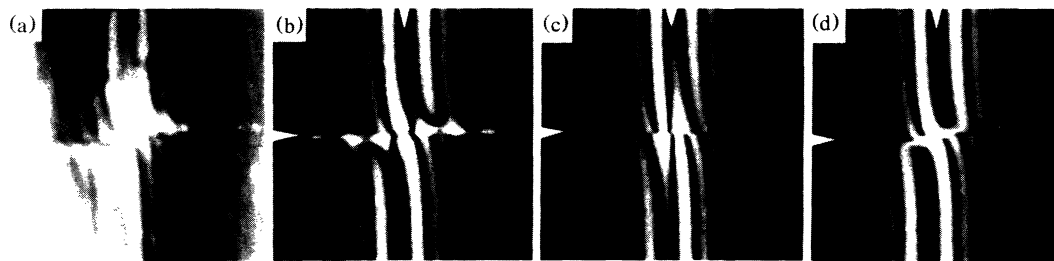


FIG. 2. (a) Large-angle $(11\bar{2}0)$ convergent-beam diffraction pattern from graphite. The bright field disk encroaches on the left of the pattern. (b),(c),(d) Computed diffraction patterns, calculated with use of exact equations, simple adiabatic approximation, and modified Bloch-wave theory, respectively. $x$ runs horizontally and $y$ vertically; the arrows mark the positions of the lines $x = 0$ and $y = 0$. See text for details.

ness parameter.[12] As $y$ increases away from the dislocation core, the planes curve less (Fig. 1) and the Hamiltonian varies increasingly slowly. Second, the relative phase of the two eigenstates is observed, rather than the separate phase of each. This follows from the boundary conditions at the entrance surface ($\theta = -1$), where $A_0 = 1$ and $A_g = 0$. A superposition of the two eigenstates is therefore created; in the adiabatic limit these propagate with equal and opposite dynamical *and* geometrical phases before giving rise to diffracted beams at the exit surface. Because the relative phase is observed it is not necessary for the path taken by the Hamiltonian to be closed. It does close at special values of $y$, when the total change in $\phi$, $\Delta\phi$, is a multiple of $2\pi$. This occurs when $1/y = \tan(2n\pi^2/\mathbf{g}\cdot\mathbf{b})$, in which case the geometrical phase (at $\theta = 1$) becomes

$$\gamma = -\frac{1}{2}\frac{2n\pi x}{(x^2+\beta^2)^{1/2}}.$$

This agrees with Berry's[1] solid-angle rule for calculating $\gamma$; our circuit corresponds to moving $n$ times around a sphere on a line of latitude at an angle $\cos^{-1}[x/(x^2+\beta^2)^{1/2}]$ from the equator. In the present case these closed paths are not special; the diffraction is calculated for all values of $y$.

In order to have an exact result with which to compare different approximations we have numerically integrated (2) for $\mathbf{g}\cdot\mathbf{b}/2\pi = 2$ and $\beta = 2.85$, with $x$ and $y$ extending over ranges $-25$ to 25 and $-4$ to 4, respectively. The result is shown in Fig. 2(b) and shows good agreement with the experimental micrograph [Fig. 2(a)]. Small differences are probably due to the dislocation being a little off center.[13] The bending of the two-beam fringes due to the long-ranged strain field is clearly seen. In the lowest-order adiabatic approximation we let the amplitude of each eigenstate remain constant. The resulting diffraction is identical to the standard two-beam case,[7] but with the geometrical phase (3) adding to the dynamical phase. The diffracted intensity becomes

$$I_g = \beta^2 \frac{\sin^2[(x^2+\beta^2)^{1/2}+\gamma]}{x^2+\beta^2}, \tag{4a}$$

where

$$\gamma = -\frac{x}{(x^2+\beta^2)^{1/2}}\frac{\mathbf{g}\cdot\mathbf{b}}{2\pi}\tan^{-1}(1/y). \tag{4b}$$

$\gamma$ therefore causes a $y$-dependent shift of the two-beam fringes, observed as a fringe bending in Fig. 2(c). Comparison with Fig. 2(b) shows that the adiabatic approximation fails both near the dislocation core ($y$ small) and near the Bragg condition ($x$ small). In both these cases off-diagonal terms cannot be ignored.[13] Away from these regions the adiabatic expressions (4) provide an excellent approximation to the exact result and we conclude that *the bending of the subsidiary fringes as the dislocation is approached is a direct consequence of the*

*geometrical phase* $\gamma$. Interestingly, these results are far from new in electron diffraction theory. The phenomenon of fringe bending has been understood for some time,[14] while the phase factor [(3) and (4b)] appears first to have been derived by Howie[15] and is discussed by several other authors.[7,16] The connection with Berry's work is, however, new.

The electron diffraction literature provides other methods for the analysis of (2) and it is interesting to reexamine these in the light of the results presented here. One of the most useful approximations is the modified Bloch-wave theory.[16] Here we apply the unitary transformation

$$\begin{bmatrix} \tilde{A}_0 \\ \tilde{A}_g \end{bmatrix} = \begin{bmatrix} e^{-i\phi/2} & 0 \\ 0 & e^{i\phi/2} \end{bmatrix} \begin{bmatrix} A_0 \\ A_g \end{bmatrix}$$

to (2), yielding

$$\frac{1}{2}\begin{bmatrix} x-\dot{\phi} & \beta \\ \beta & -x+\dot{\phi} \end{bmatrix}\begin{bmatrix} \tilde{A}_0 \\ \tilde{A}_g \end{bmatrix} = -i\frac{d}{d\theta}\begin{bmatrix} \tilde{A}_0 \\ \tilde{A}_g \end{bmatrix}. \tag{5}$$

In the adiabatic limit, (5) has no geometrical phase (the Hamiltonian is real) and the off-diagonal, nonadiabatic terms are proportional to $\ddot{\phi}$, while for the original Hamiltonian they are proportional to $\dot{\phi}$. In other words, the error in making an adiabatic approximation now lies in ignoring the curvature of the diffracting planes rather than their slope.[16] The phase now appears to be entirely dynamical in origin and for the two eigenstates (i.e., modified Bloch waves) is given by

$$\pm\frac{1}{2}\int_{-1}^{1} d\theta[(x-\dot{\phi})^2+\beta^2]^{1/2}. \tag{6}$$

The transformation leading to (5) is not of the type considered by Berry[12] in setting up an adiabatic iteration scheme because it is not based on the parallel-transport rule. Also, $\dot{\phi}$ does not go to zero at the boundaries, and so the initial eigenstates of (5) are different from those of (2). The connection with Berry's work can, however, be seen if we expand the integrand in (6), assuming that $\dot{\phi}$ is small. To lowest order (6) reduces to the argument of the sine in (4a), while the first correction agrees with that in Berry's[12] Eq. (45). The adiabatic approximation to (5) gives the diffraction pattern shown in Fig. 2(d). The improvement over the simplest adiabatic result [Fig. 2(c)] is considerable; indeed differences with the exact result are apparent only very close to the dislocation core.

In conclusion, we have shown that electron diffraction provides a particularly clear demonstration of the geometrical phase. For simplicity we have concentrated on the special case of a screw dislocation in the center of a specimen, but a similar analysis can be applied to off-center screw dislocations, other sorts of dislocation, and indeed any lattice defect which induces a long-ranged strain field. The phase $\gamma$ which appears in (4) is depen-

dent on the total change of structure factor phase, $\Delta\phi$, which occurs in crossing the crystal. Provided the diffracting planes do not return to their original position at the exit surface of the crystal $\Delta\phi$ will be nonzero, leading to a nonzero geometrical phase and diffraction effects of the type discussed above.

[1] M. V. Berry, Proc. Roy. Soc. London A **392**, 45 (1984).

[2] A. Tomita and R. Y. Chiao, Phys. Rev. Lett. **57**, 937 (1986); R. Simon, H. J. Kimble, and E. C. G. Sudarshan, Phys. Rev. Lett. **61**, 19 (1988).

[3] T. Bitter and D. Dubbers, Phys. Rev. Lett. **59**, 251 (1987).

[4] R. Tycko, Phys. Rev. Lett. **58**, 2281 (1987).

[5] G. Delacrétaz, E. R. Grant, R. L. Whetten, L. Wöste, and J. W. Zwanziger, Phys. Rev. Lett. **56**, 2598 (1986); F. S. Ham, Phys. Rev. Lett. **58**, 725 (1987).

[6] J. W. Steeds, *Anisotropic Elasticity Theory of Dislocations* (Clarendon, Oxford, 1973).

[7] A. Howie and M. J. Whelan, Proc. Roy. Soc. London A **263**, 217 (1961); P. B. Hirsch, A. Howie, R. B. Nicholson, D. W. Pashley, and M. J. Whelan, *Electron Microscopy of Thin Crystals* (Krieger, New York, 1977); C. J. Humphreys, Rep. Prog. Phys. **42**, 1825 (1979).

[8] A. Howie and Z. S. Basinski, Philos. Mag. **17**, 1039 (1968).

[9] M. Tanaka and M. Terauchi, *Convergent Beam Electron Diffraction* (JEOL, Tokyo, 1985).

[10] J. A. Eades and C. J. Keily, in *Electron Microscopy and Analysis—1987*, edited by L. M. Brown, IOP Conference Proceedings No. 90 (Institute of Physics, Bristol and London, 1987), p. 109; D. Cherns, C. J. Keily, and A. R. Preston, Ultramicroscopy **24**, 355 (1988); M. Tanaka, M. Terauchi, and T. Kaneyama, *Convergent Beam Electron Diffraction II* (JEOL, Tokyo, 1988); D. Cherns and A. R. Preston, J. Electron Microsc. Tech. (to be published).

[11] B. Simon, Phys. Rev. Lett. **51**, 2167 (1983).

[12] M. V. Berry, Proc. Roy. Soc. London A **414**, 31 (1987).

[13] D. M. Bird and A. R. Preston, to be published.

[14] N. Kato, Acta Crystallogr. **16**, 282 (1963); W. Bollmann, Philos. Mag. **13**, 935 (1966); F. W. Schapink, Phys. Status Solidi (a) **29**, 623 (1975).

[15] A. Howie, Proc. Roy. Soc. London A **271**, 268 (1963).

[16] M. Wilkens, Phys. Status Solidi **6**, 939 (1964); M. Wilkens, M. Rühle, and F. Haüssermann, Phys. Status Solidi **22**, 689 (1967); M. Wilkens, K. H. Katerbau, and M. Rühle, Z. Naturforsch. a **28**, 681 (1973).

FIG. 2. (a) Large-angle $(11\bar{2}0)$ convergent-beam diffraction pattern from graphite. The bright field disk encroaches on the left of the pattern. (b),(c),(d) Computed diffraction patterns, calculated with use of exact equations, simple adiabatic approximation, and modified Bloch-wave theory, respectively. $x$ runs horizontally and $y$ vertically; the arrows mark the positions of the lines $x=0$ and $y=0$. See text for details.